CHAPTER 144

SAND TRANSPORT ON THE SHOREFACE OF THE HOLLAND COAST

The Dutch Coast: Paper No. 5

J.A. Roelvink[1] and M.J.F. Stive[1]

Summary

Yearly averaged transport vectors have been computed along a number of rays, perpendicular to the coast, on the shoreface of the Holland coast. Variation in time and space of wave conditions, tidal flow and long-term average near-bottom flows are considered in fine detail. Special attention is paid to various correlations, both between different velocity components and between velocity and water level, as these correlations play a major role in determining direction and magnitude of net transports. Calibration is performed against both long-term and short-term observations of developments. The resulting transport pattern helps to explain some observed large-scale developments of the Dutch coast.

1. Introduction

The Coastal Genesis Research Programma of Rijkswaterstaat aims to identify geomorphological processes that determine the long-term, large-scale development of the Dutch coast. To this end a collection of interdisciplinary projects has been set up among geologists, geographers and civil engineers of Rijkswaterstaat, National Geology Department, DELFT HYDRAULICS and several universities. In 1988 and 1989 Rijkswaterstaat asked the researchers involved to contribute to supporting studies for a Coastal Defence Study, aiming to develop an overall coastal defence strategy for the Netherlands (Louisse and Kuik, Paper No. 1, these proceedings). The results presented here were generated for this study.

The goal of this study is to provide backing for conceptual large scale evolution models of the Dutch coast, developed in the framework of the Coastal Genesis Programme (see Stive et al, 1990). These models can then be used to improve predictions of the coastal developments, required by the Coastal Management Study. More specifically, this study should provide an estimate of the large-scale net transport pattern on the shoreface, and identify the relative importance of the mechanisms contributing to this pattern.

1 DELFT HYDRAULICS, P.O. Box 152, 8300 AD Emmeloord, The Netherlands

The general approach followed in this study is, to estimate hydraulic conditions in a number of points, and to analyze the resulting transport vectors in these points. As the interest is focussed on large-scale trends, estimates of the variation of hydraulic conditions along the coast can be based on the data from existing measuring stations. The variation of conditions perpendicular to the coast can be computed (on this large scale) with ray models or empirical formulations. Special care must be given to correlations between variables and non-linear effects; the importance of many of these aspects has been shown, among others, by Roelvink and Stive (1989). As the net transport in the area of interest is generally small compared to the amplitudes of the tidal and orbital contributions, second-order effects are of major importance.

2. Model assumptions

The basic assumptions which are made are, that the deep water (approx. 20 m water depth) wave and current conditions vary slowly along the Holland coast, and that on a longshore scale of tens of kilometres the depth contours are approximately parallel. Under these conditions, the problem is reduced to a one-dimensional problem which is solved for a limited number of cross-shore sections. The spatial resolution is thus limited, in accordance with the large-scale concept that the model is a part of.

In such a large-scale model, the relevant time-scale is at least in the order of years. However, in order to arrive at estimates of yearly-averaged transports, the transport at a given point must be correctly integrated over a number of shorter time-scales: the short-wave time-scale, the wave-group scale, the tidal-scale, the storm-scale and the seasonal variations. The variations on all these time-scales and the interactions between some of them potentially cause net transports. This means that we have to go back some time-scales in order to produce the long-term parameter: 'yearly-averaged transport'.

3. Analysis of relevant interactions

For the computations of sediment transport due to a combination of waves and currents, in both wave- and current direction, one of the few (practically suitable) available formulations is that of Bailard (1981) after the concept by Bagnold (1966). This formulation has proved reasonably accurate in the case of cross-shore transport (Roelvink & Stive, 1988; Ribberink & Al Salem, 1990). It is conceptually simple and is able to combine transport contributions from different directions and on different time-scales.

The formulation describes the transport as a function of the instantaneous near-bottom velocity at a certain reference level:

$$\langle \vec{q}_x \rangle = \frac{c_f}{\Delta g N} \frac{\varepsilon_B}{\tan\phi} \left[\langle |\vec{u}|^2 \vec{u}_x \rangle - \frac{\tan\beta_x}{\tan\phi} \langle |\vec{u}|^3 \rangle \right] + \\ + \frac{c_f}{\Delta g N} \frac{\varepsilon_s}{w} \left[\langle |\vec{u}|^3 \vec{u}_x \rangle - \frac{\varepsilon_s}{w} \tan\beta_x \langle |\vec{u}|^5 \rangle \right] \qquad (1)$$

$$\langle \vec{q}_y \rangle = \frac{c_f}{\Delta g N} \frac{\varepsilon_B}{\tan\phi} \left[\langle |\vec{u}|^2 \vec{u}_y \rangle - \frac{\tan\beta_y}{\tan\phi} \langle |\vec{u}|^3 \rangle \right] +$$
$$+ \frac{c_f}{\Delta g N} \frac{\varepsilon_s}{w} \left[\langle |\vec{u}|^3 \vec{u}_y \rangle - \frac{\varepsilon_s}{w} \tan\beta_y \langle |\vec{u}|^5 \rangle \right]$$

where x,y are two arbitrary directions perpendicular to each other, q is the total volume transport, $\vec{u}$ is the instantaneous total velocity vector, c_f a roughness coefficient, Δ the relative density, g the acceleration of gravity, N the fraction of sediment relatieve to total volume, w the fall velocity, ε_B and ε_s efficiency factors (calibration constants) and $\tan\beta$ the bottom slope. The $\langle\ \rangle$ indicate averaging over time, the averaged powers of the velocity are also called 'velocity moments'.

From flume and wave tunnel experiments (Ribberink & Al Salem, 1990) it follows that the term with the power of 3 is the dominant term in the equation. For a first analysis we can therefore use:

$$\langle \vec{q} \rangle = A \langle |\vec{u}|^2 \vec{u} \rangle \qquad (2)$$

Now we can estimate the relative importance of contributions to the transport on different time-scales, by decomposing the velocity vector into components which act on the time-scales from short waves to storm periods.

$$\vec{u} = \vec{u}_{nL} + \vec{u}_{nC} + \vec{u}_t + \vec{u}_l + \vec{u}_s \qquad (3)$$

where:

$\vec{u}_{nL} = u_{nL} \begin{bmatrix} 1 \\ 0 \end{bmatrix}$ = net longshore current,

$\vec{u}_{nC} = u_{nC} \begin{bmatrix} 1 \\ 0 \end{bmatrix}$ = net cross-shore current,

$\vec{u}_t = u_t \begin{bmatrix} 1 \\ 0 \end{bmatrix}$ = tidal current,

$\vec{u}_l = u_l \begin{bmatrix} \cos\alpha \\ \sin\alpha_w \end{bmatrix}$ = long-wave motion,

$\vec{u}_s = u_s \begin{bmatrix} \cos\alpha \\ \sin\alpha_w \end{bmatrix}$ = short-wave motion.

All velocities are taken here at a near bottom reference level; the x-direction is taken alongshore, and the y-direction onshore, α_w is the angle between the longshore direction and the direction of wave propagation. Both long waves and short waves are assumed to have the same dominant direction.

The term $\vec{u}$ in equation (2) can be substituted by equation (3); after some simple algebraic manipulations and neglecting what we estimate to be small terms, we then find:

$$
\begin{aligned}
\langle|\vec{u}|^2\vec{u}\rangle = {} & \langle u_{nL}u_t^2\rangle \begin{bmatrix}3\\0\end{bmatrix} + && \text{net longshore - tidal current interaction}\\
& + \langle u_{nC}u_t^2\rangle \begin{bmatrix}0\\1\end{bmatrix} + && \text{net cross-shore - tidal current interaction}\\
& + \langle u_{nL}u_s^2\rangle \begin{bmatrix}\cos 2\alpha + 2\\ \sin 2\alpha\end{bmatrix} + && \text{net longshore - short wave interaction}\\
& + \langle u_{nC}u_s^2\rangle \begin{bmatrix}\sin 2\alpha\\ 2 - \cos\alpha_w\end{bmatrix} + && \text{net cross-shore - short wave interaction}\\
& + \langle u_t^3\rangle \begin{bmatrix}1\\0\end{bmatrix} + && \text{tidal current asymmetry}\\
& + \langle u_t u_s^2\rangle \begin{bmatrix}\cos 2\alpha_w + 2\\ \sin 2\alpha_w\end{bmatrix} + && \text{tide - short wave interaction}\\
& + \langle u_l u_s^2\rangle \begin{bmatrix}3\cos\alpha_w\\ 3\sin\alpha_w\end{bmatrix} + && \text{long - short wave interaction}\\
& + \langle u_s^3\rangle \begin{bmatrix}\cos\alpha_w\\ \sin\alpha_w\end{bmatrix} + && \text{short wave asymmetry} \qquad (4)
\end{aligned}
$$

The relative importance and some characteristics of these terms are described below.

Net longshore-tidal current interaction

The two components are generally uncorrelated. As the variance of the tidal velocity is relatively high, a small net current can cause significant transport: the tide stirs up sediment which is advected by the net current.

Net cross-shore-tidal current interaction

This term is similar to the previous one. Even though the net cross-shore current may be small, it may give an important contribution in combination with the stirring up due to the tidal velocity.

Net longshore - short wave interaction

The components in this term are highly correlated. Two mechanisms are responsible for this: during storms the wind drives both currents and waves, and, more directly, the waves drive a net longshore current.
An interesting side-effect of the interaction term is, that it is not directed in longshore direction, but has a deviation which for angles $< 90^\circ$ (which is generally the case) is directed onshore.

Net cross-shore - short wave interaction

These components are also highly correlated. During storms, wind- and wave -driven cross-shore currents occur near the bottom, which are generally directed offshore; during calm weather these currents tend to be directed onshore.

Tidal current asymmetry

Along the Holland coast, the tide manifests itself as a northward propagating wave, where the M2 and M4 components are more or

less in phase. This causes an asymmetric velocity; the highest velocity occurs in northward direction. Due to this, the term causes a net northward transport component.

Tide - short wave interaction

The tide and the short waves interact through the water level variation. Two mechanisms play a role. The most important one is, that the water level influences the orbital velocities: the greater the water depth, the smaller the orbital velocity. As the lowest water level occurs during South flowing current, this mechanism causes a net southward effect. On the other hand, a lower water level implies more wave dissipation due to friction and breaking, which reduces the wave height and thus the orbital velocity. This effect reduces the net southward effect somewhat.

Long - short wave interaction

In groupy waves variations in radiation stress occur which drive long waves ('bound long waves', Lonquet-Higgins & Stewart, 1964). Outside the breaker-zone these long waves are generally in counterphase with the varying wave energy, thus, when the highest waves occur, the long-wave velocity is directed offshore. Due to this, a net offshore interaction term arises (Shi and Larsen, 1984).

Short wave asymmetry

Due to non-linearity, the orbital velocity under short waves is asymmetric in time; the velocities under wave crests are higher than those under the troughs. This leads to a large transport term directed onshore.

4. Model formulation

Based upon the above analysis of the important terms that contribute to the yearly averaged transport, we may conclude that the interaction between the tidal motion and the wave motion is such that we have to take this fully into account. This is done in the following way.

The offshore tidal motion is schematized to a number of 12 steps within a representative tidal cycle; The deep water velocities and water levels at a given location are determined by interpolating tidal coefficients in space between measuring stations. The variation in offshore wave conditions is represented by a climate of 80 combinations of wave heights and directions, each combination with its representative wave period and offshore water level set-up. The deep water wave climate at a given location is also obtained by interpolation in space of measured wave climates, based on 10 years of observations at three measuring stations at 20 m water depth.
This leads, for a given location, to 960 sets of deep water boundary conditions.

Each of these boundary conditions is then used in a computation of depth-mean wave and current parameters along a line perpendicular to the depth contours, with the help of one-dimensional models.

From these depth-mean parameters, the near-bottom quasi-steady velocity and the relevant velocity moments due to wave asymmetry and long wave - short wave interactions are computed. These are combined

to yield the total velocity moment vectors which are required by the transport model according to equation (1).

In a number of points along the cross-shore line, the thus computed transport vectors are integrated over all combinations; taking into account the frequency of occurrence of each combination. This then leads to the yearly-averaged transport vector in each point along the line.

In the following, the formulations used to achieve this are summarized.

Cross-shore variation of wave parameters

The wave energy decay model formulated by Battjes & Janssen (1978), with the parametrizations from Battjes & Stive (1985) is used:

$$\frac{\partial}{\partial x}\left(E\, C_g \cos\theta_w\right) = -D \tag{5}$$

$$\frac{\sin\theta_w}{C} = \frac{\sin\theta_{w,o}}{C_o} \tag{6}$$

$$\rho g h \frac{\partial \bar{\eta}}{\partial x} = -\frac{\partial}{\partial x} S_{xx}$$

Here, E is the wave energy, C_g the group velocity, θ_w the angle of the wave propagation direction to the shore normal, D the dissipation due to bottom friction and breaking, C the phase velocity, ρ the density of water, h the total mean water depth, $\bar{\eta}$ the water level set-up and S_{xx} the radiation stress. The subscript 0 denotes deep-water (most offshore location).

Cross-shore variation of current parameters

For the tidal current, the assumption is used that the alongshore pressure gradient is constant along the cross-shore line, and is compensated by bottom friction. Using the Chézy friction-law, we then find:

$$U_t = U_{t,o} \frac{C_h}{C_{h_o}} \left[\frac{h}{h_o}\right]^{0.5} \tag{7}$$

where $C_h = 18 \log \frac{12\, h}{k_s}$ is the Chézy friction coefficient, k_s is the bottom roughness, and $\bar{U}_t$ the depth-mean tidal current.

For the wave-driven longshore current, the cross-shore gradient of the alongshore component of the radiation stress S_{yx} is assumed to be compensated by the bottom shear stress due to current and waves. The radiation stress gradient is modelled according to Dingemans et al (1987).

$$-\frac{\partial}{\partial x} S_{yx} = \frac{D}{C} \sin\theta_w \tag{8}$$

and for the bottom shear stress τ_y a linearized form is used:

$$\tau_y = \rho\, C_f\, \bar{U}_l \langle |U_{orb}| \rangle \tag{9}$$

where $\bar{U}_1$ is the longshore current, $<|U_{orb}|>$ the mean value of the absolute magnitude of the orbital velocity and C_f a friction coefficient.
From (8) and (9), $\bar{U}_1$ can be solved.

Near-bottom quasi-steady velocity

Both the tidal current velocity and the wave-driven longshore current at a reference level near the bottom are derived from the depth-mean velocity by assuming a logarithmic profile.

The wave-driven cross-shore current is computed by the method given in Stive & De Vriend (1987); the formulations will not be repeated here.

An empirically found near-bottom long-term net moment as reported in Borst (1987) was added to the near-bottom velocity components.

Velocity moments of wave motions

The relevant velocity moments due to short wave asymmetry and long wave-short wave interaction can be estimated from the rms wave height, the peak period and the water depth by using the method outlined in Roelvink & Stive (1989). For the short wave asymmetry, the method is based on high order non-linear wave theory; for the long wave effects a simple bound long wave model is used.

Total quasi-steady velocity moments

The near-bottom quasi-steady current and the (also quasi-steady) velocity moments of the wave motions are combined to produce the total quasi-steady velocity moments and moment vectors for the given combination of tidal phase and wave condition. This involves lengthy expressions based on Taylor expansion in two directions, which are given in the original report (Roelvink & Stive, 1989a).

5. Results

Computations with this model were carried out for four rays along the Holland coast. The resulting large-scale transport pattern is shown in Figure 1. The arrows indicating the relative strength of the yearly averaged transport are located at 20 m, 15 m, 10 m and 8 m respectively.

Because of the simplicity of the used models, considerable errors are possible. Therefore, an overall calibration of the transports was performed against observed large-scale phenomena. The observations taken into account are:

- The long-term flattening of the middle shoreface, as evident from a steady shoreward migration of the -10 m depth contour line over the last 90 years.

- The order of magnitude of the net longshore transport in the surfzone as a function of the orientation of the coastline. This has been the subject of much studies based on observed morphologic developments, most recently by Dijkman et al (1990).

- The observed northward migration of the navigation channel off IJmuiden Harbour (see Van Alphen et al, 1990).

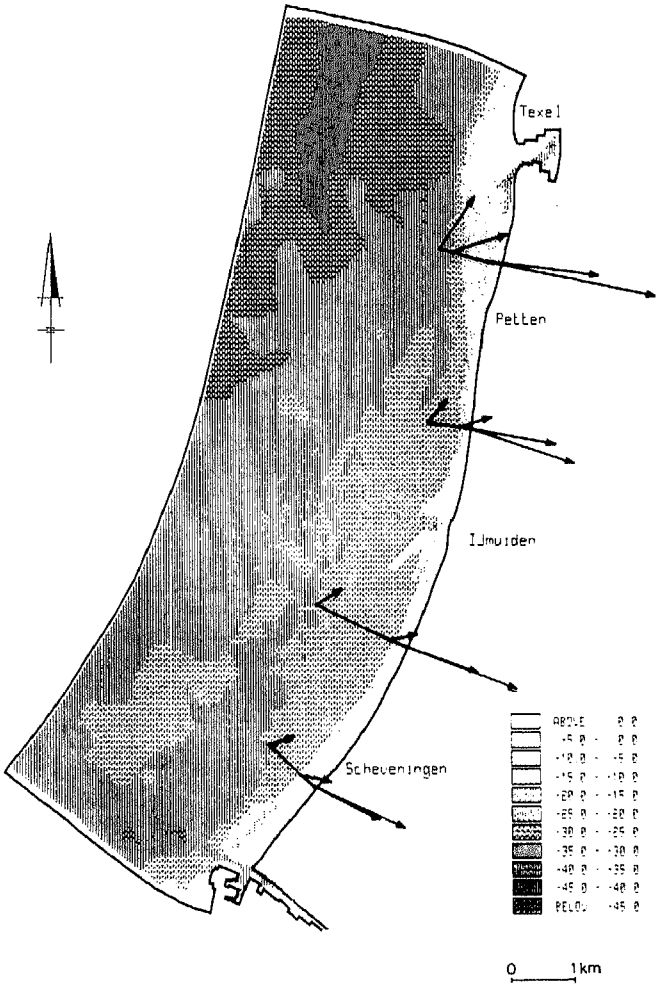

Figure 1 Net transport vectors, uncalibrated

These observations have led to an adjustment of the transport rates; cross-shore transport were reduced by a factor of 2, whereas the longshore transport had to be multiplied by a factor of 2.

Although a factor of 2 in transport formulations is a minor adjustment, the fact that different factors had to be used for longshore and cross-shore transport is worrying and may be an indication that the transport model, which has proved to perform reasonably for wave-induced transport, does not perform so well in combinations of waves and currents.

The calibrated large-scale transport pattern is shown in Fig. 2. The picture shows a transition from the tide-dominated transport (mainly caused by the coupling of the M2 and M4 components) to wave-dominated transport. Towards the -8 m depth contours, the cross-shore transport increases as a result of increasing wave-induced streaming and short wave asymmetry; the longshore transport also becomes more wave-dominated and shows a clear dependance on the coast orientation.

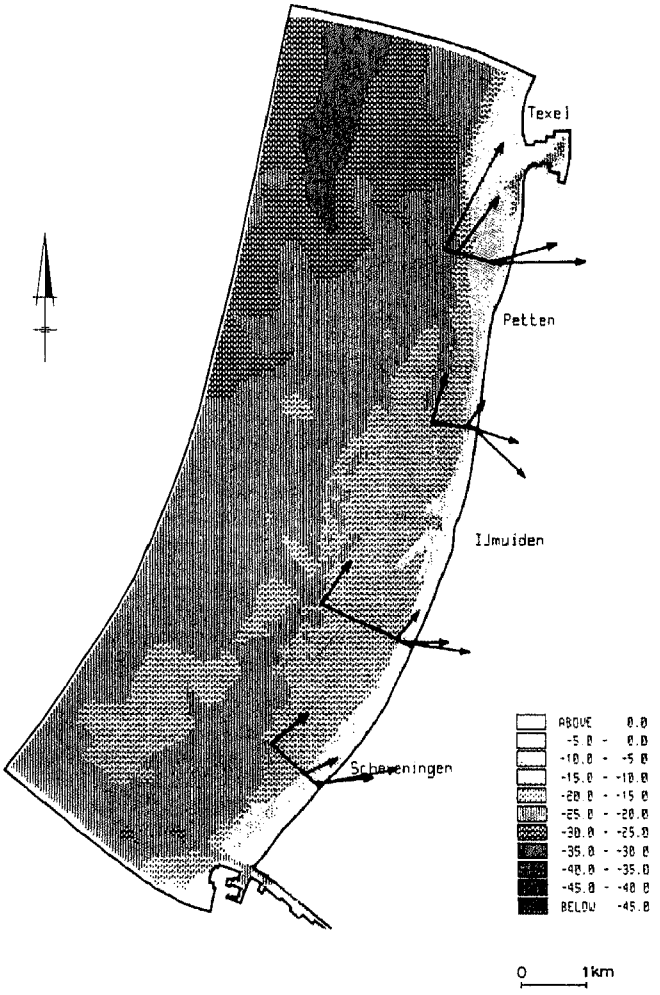

Figure 2 Net transport vectors, calibrated

In Fig. 3a, the variation of the net near-bottom velocity and transport, averaged over all wave conditions, as a function of the tidal phase is given for the most northern ray, at a depth of 18 m;

in Fig. 3b, the same is done at a depth of 10 m. This clearly shows the dominance of the tidal transport in deep water: the transport direction closely follows the tidal velocity; also, the transport increases non-linearly with increasing tidal velocity. At a depth of 10 m, the picture is quite different. The transport has a significant onshore component; also, the dependance of the transport on the tidal velocity is almost linear, which indicates that the waves do most of the stirring of sediment, whereas the tidal velocity merely advects this sediment.

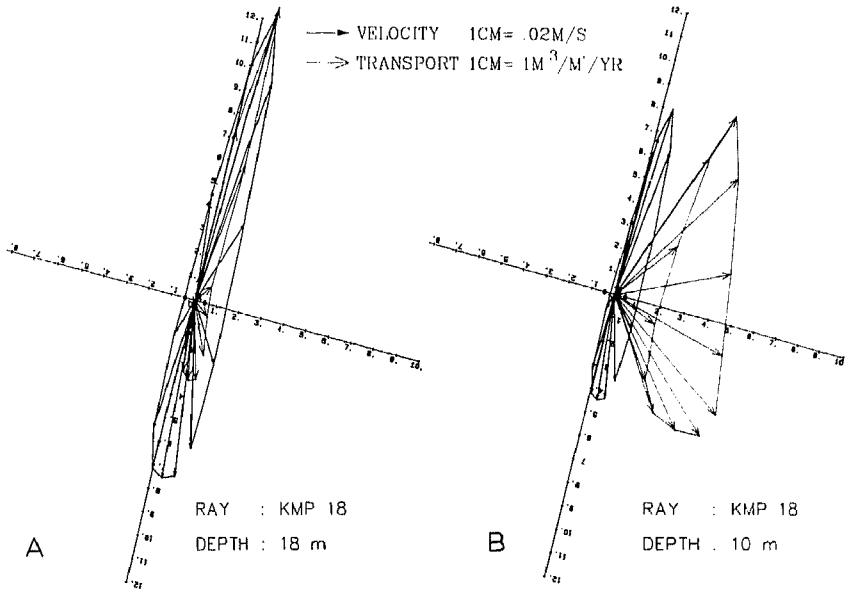

Figure 3 Velocity and transport per tidal phase average over all wave conditions

As an illustration of the variation of the cross-shore transport with water depth, the computed cross-shore transports are plotted against depth in Fig. 4. There is a sharp increase in onshore transport towards the -8 m line. Between approx. 6 m and 10 m water depth, there is a transition from the highly dynamic 'active zone' to the morphologically rather in-active shoreface (see Stive et al, Paper No. 9, these proceedings); therefore, the limit of application of this model also lies somewhere in this transition zone. An important conclusion that can be drawn from Figure 4 is, that for the Holland coast the shoreface acts as a significant source of sand to the 'active zone'.

In Figure 5, the cross-shore transport gradients are shown as a function of depth. These gradients scale directly with the propagation speed of depth contour lines. It follows that the 10 m depth contour moves shoreward at a speed of approx. 2 m per year, which is in accordance with observations.

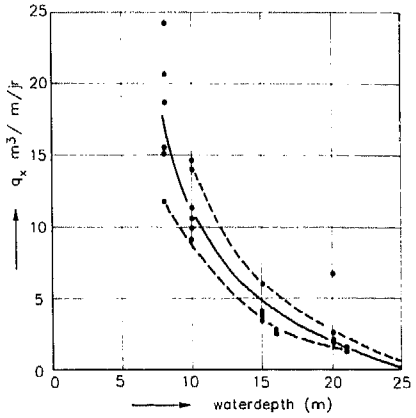

Figure 4 Net cross-shore transport vs. water depth

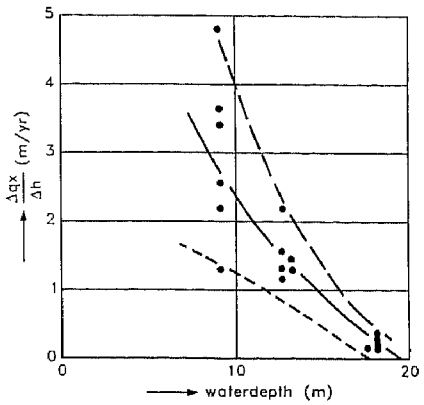

Figure 5 Net cross-shore transport gradient vs. water depth

6. Sensitivity analysis

As the value of a number of coefficients in the model and some hydrodynamic input data was rather uncertain, a sensitivity analysis was carried out in order to estimate the total errors in the computed transport rates. This was done in the following way: for a number of input values, the standard deviation was estimated. The effect on the transport rates was assessed by consecutively adding or subtracting this standard deviation from the expected value of the inputs. The errors in the transport rates due to these errors were then squared and added, and the square root was taken to yield an estimate of the total percentage error. This method is known as the 'mean value' approximation. Here we shall not go into all details of the analysis, but simply present the final result in Fig. 6 for the cross-shore transport, and Fig. 7 for the longshore transport.

The errors in the longshore transport increase in seaward direction, up to around 100%. This is mainly due to the fact, that the net transport rate in deep water is very small compared to the gross transport rates, which increases the sensitivity of the output substantially.

The errors in the cross-shore transport also increase in seaward direction, mainly due to uncertainties in the near-bottom net currents.

7. Discussion

The model presented here has been a useful tool in comparing the relative importance of a number of interacting transport mechanisms on the shoreface. After calibration, a plausible transport pattern emerges which in some aspects helps the understanding of the observed large-scale morphologic developments.

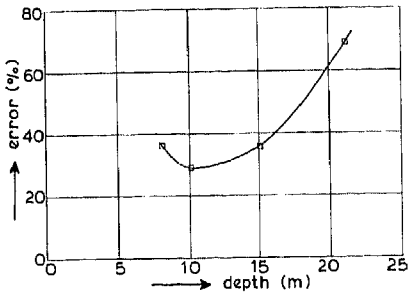

Figure 6 Estimated total error; cross-shore transport

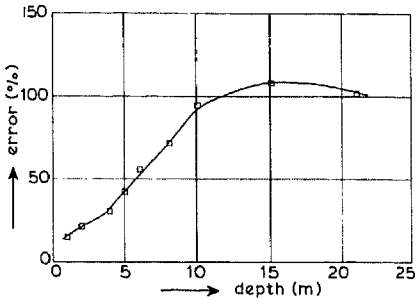

Figure 7 Estimated total error; long-shore transport

However, the model has some serious limitations: many of the processes incorporated in it are crudely schematized, and much about the hydraulic conditions, especially in deeper water, is uncertain.

One might therefore agree that, given these uncertainties, it might be better not to build such a model at all. This is not our opinion; as long as the limitations are stated clearly, models like this are useful tools of analysis and at least provide an educated 'best guess' of what is happening.

References

Van Alphen, J.S.L.J., C.J. Louisse, F.P. Hallie, J.S. Ribberink and J.A. Roelvink, (1990).
Offshore sand extraction and nearshore profile nourishment.
The Dutch coast: Paper No. 12.
Proc. 22nd ICCE, Delft, The Netherlands, 1990.

Bagnold, R.A. (1966).
An approach to the sediment transport problem from general physics.
U.S. Geol. Surv. Prof. Pap. 422-I, 1966.

Bailard, J.A. (1981).
An energetics total load sediment transport model for a plane sloping beach.
J. Geophys. Res., Vol. 86, No. C11, pp. 10,938-10,954, 1981.

Battjes, J.A. and J.P.F.M. Janssen (1978).
Energy loss and set-up due to breaking in random waves.
Proc. 16th ICCE, pp. 569-87, 1978.

Battjes, J.A. and M.J.F. Stive (1985).
Calibration and verification of a dissipation model for random breaking waves.
J. Geophys. Res., Vol. 90, pp. 9159-67.

Borst, J.C. (1987).
Verkennende beschrijving van het stroomklimaat in het kustvak Delfland (in Dutch).
Rijkswaterstaat, Nota GWAO-87.477, The Hague, The Netherlands.

Dingemans, M.W., A.C. Radder, H.J. de Vriend (1987).
Computation of the driving forces of wave-induced currents.
Coastal Eng. 11 (1987) 539-563, Elsevier, Amsterdam, The Netherlands.

Dijkman, M.J., W.T. Bakker, J.H. de Vroeg (1990).
Prediction of coastline evolution for specific parts of the Holland coast. The Dutch coast: Paper No. 7.
Proc. 22nd ICCE, Delft, The Netherlands, 1990.

Lonquet-Higgins, M.S. and R.W. Stewart (1964).
Radiation stress in water waves; a physical discussion, with applications.
Deep-Sea Res., 1964, Vol. 11, pp. 529-562, Pergamoma, Great Britain.

Ribberink, J.S. and A. Al Salem (1990).
Bedforms, sediment concentrations and sediment transport in simulated wave conditions.
Proc. 22nd ICCE, Delft, The Netherlands, 1990.

Roelvink, J.A. and M.J.F. Stive (1988).
Large-scale tests of cross-shore sediment transport on the upper shoreface.
Symp. Math. Modelling of Sed. Transp. in the Coastal Zone, Copenhagen, 1988.

Roelvink, J.A. and M.J.F. Stive (1989).
Bar-generating cross-shore flow mechanisms on a beach.
J. Geophys. Res., Vol. 94, C4, pp. 4785-4800, 1989.

Roelvink, J.A. and M.J.F. Stive (1989a).
Voorspelling ontwikkeling kustlijn 1990-2090, fase 3; deelrapport 3.4: initieel sedimenttransportmodel Hollandse kust.
DELFT HYDRAULICS, report H825, Delft, Sept. 1989 (in Dutch).

Shi, N.C. and L.H. Larsen (1984).
Reverse sediment transport induced by amplitude-modulated waves.
Mar. Geol., 54: 181-200.

Stive, M.J.F., J.A. Roelvink and H.J. de Vriend (1990).
Large-scale coastal evolution concept. The Dutch coast: Paper No. 9.
Proc. 22nd ICCE, Delft, The Netherlands, 1990.

Stive, M.J.F. and H.J. de Vriend (1987).
Quasi-3d current modelling: wave-induced secondary current.
ASCE Specially Conf. "Coastal Hydrodynamics", Delaware, 1987.